Supporting Information

Microporous metal-organic frameworks with hydrophilic and hydrophobic pores for efficient separation of CH_4/N_2 mixture

Miao Chang, Yingjie Zhao, Qingyuan Yang, Dahuan Liu*

State Key Laboratory of Organic-Inorganic Composites, Beijing University of Chemical Technology, Beijing 100029, China

E-mail: liudh@mail.buct.edu.cn

Table of Contents

S1. Calculation of the *SSP*

Sorbent selection parameter (*SSP*) can be calculated as:

$$SSP = \frac{\left(S_{i/j}^{ads}\right)^2}{\left(S_{i/j}^{des}\right)} \times \frac{\left(N_i^{ads} - N_i^{des}\right)}{\left(N_j^{ads} - N_j^{des}\right)}$$

where $S_{i/j}^{ads}$ and $S_{i/j}^{des}$ are the selectivities of *i* and *j* components, N^{ads} and N^{des} are the adsorption capacity. The superscripts of "ads" and "des" represent the adsorption and desorption process, respectively.

S2. Calculations of IAST and Henry's law ideal selectivity

The pure single component isotherms of CH_4 and N_2 (CH_4 /N_2 (50/50, v/v)) at 298 K were fitted to the dual-site Langmuir equation：

$$y = (p_1 \times x/p_2 + x) + (p_3 \times x/p_4 + x)$$

The equilibrium composition of the CH_4 /N_2 mixture is 9.14: 0.85. The calculated IAST selectivities are about 10.8-11.5 and 10.8 at the range of tested pressures and 1.0 bar, respectively.

Table S1. The fitted parameters by using the dual-site Langmuir model based on the pure single-component isotherms data of CH_4 and N_2 in Cu-MOF at 298 K.

	298 K	
parameters	CH_4	N_2
P_1	33.693	56.311
P_2	1.300	24.852
P_3	0.00370	0.0456
P_4	1.300	24.853
R^2	0.99992	0.98472

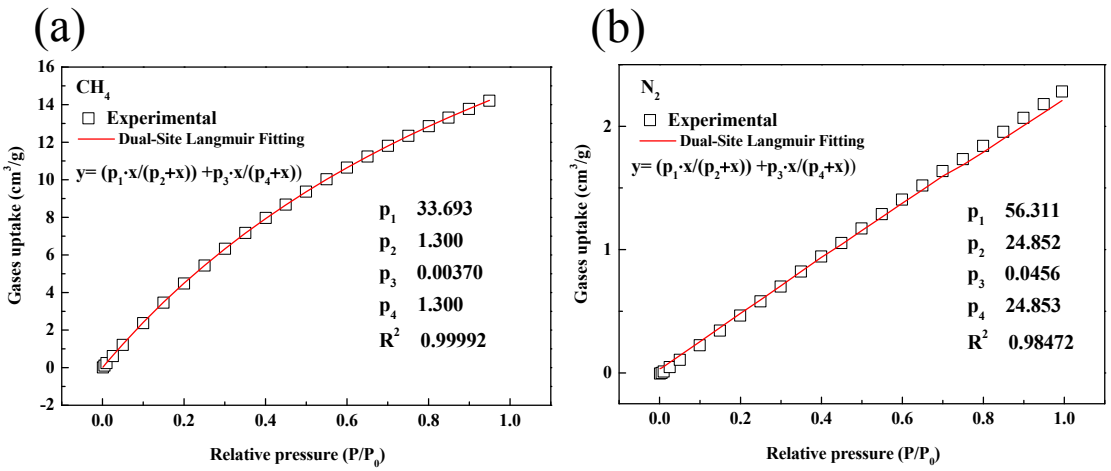

Figure S1. Fitting of the CH_4 (a) and N_2 (b) adsorption data of Cu-MOF at 298 K using dual-site Langmuir model

The pure single component isotherms of CH_4 and N_2 (CH_4 /N_2 (50/50, v/v)) at 298 K were fitted to the single-site Langmuir Freundlich equation：

$$y = (p_1 \times p_2 \times x^{N_1}/(1 + p_2 \times x^{N_1}))$$

The equilibrium composition of the CH_4 /N_2 mixture is 8.79: 0.7864. The calculated IAST selectivities are about 10.67-12.66 and 11.18 at the range of tested pressures and 1.0 bar, respectively.

Table S2. The fitted parameters by using the single-site Langmuir Freundlich model based on the pure single-component isotherms data of CH_4 and N_2 in Cu-MOF at 298 K.

	298 K	
parameters	CH_4	N_2
P_1	32.685	17.869
P_2	0.769	0.143
N_1	1.000	1.058
R^2	0.99995	0.99995

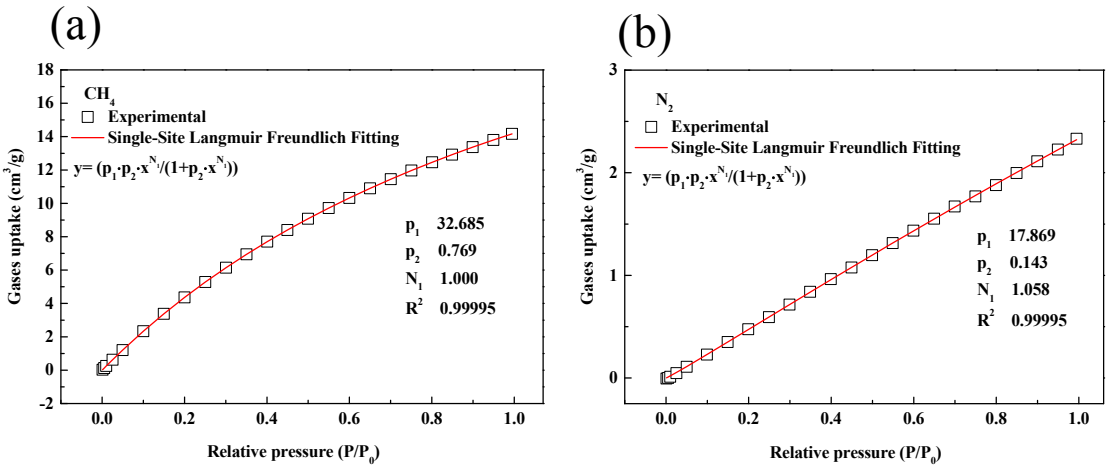

Figure S2. Fitting of the CH_4 (a) and N_2 (b) adsorption data of Cu-MOF at 298 K using single-site Langmuir Freundlich model.

The pure single component isotherms of CH_4 and N_2 (CH_4 /N_2 (50/50, v/v)) at 298 K were fitted to the dual-site Langmuir Freundlich equation：

$$y = (p_1 \times p_2 \times x^{N_1}/(1 + p_2 \times x^{N_1})) + p_3 \times p_4 \times x^{N_2}/(1 + p_4 \times x^{N_2}))$$

The equilibrium composition of the CH_4 /N_2 mixture is 8.7132: 0.7819. The calculated IAST selectivities are about 10.00-12.67 and 11.14 at the range of tested pressures and 1.0 bar, respectively.

Table S3. The fitted parameters by using the dual-site Langmuir Freundlich model based on the pure single-component isotherms data of CH_4 and N_2 in Cu-MOF at 298 K.

	298 K	
parameters	CH_4	N_2
P_1	0.0000542	12.990
P_2	40.900	0.223
N_1	1.273	1.087
P_3	32.685	0.0533
P_4	0.769	2.348
N_2	1.000	18.491
R^2	0.99994	0.99997

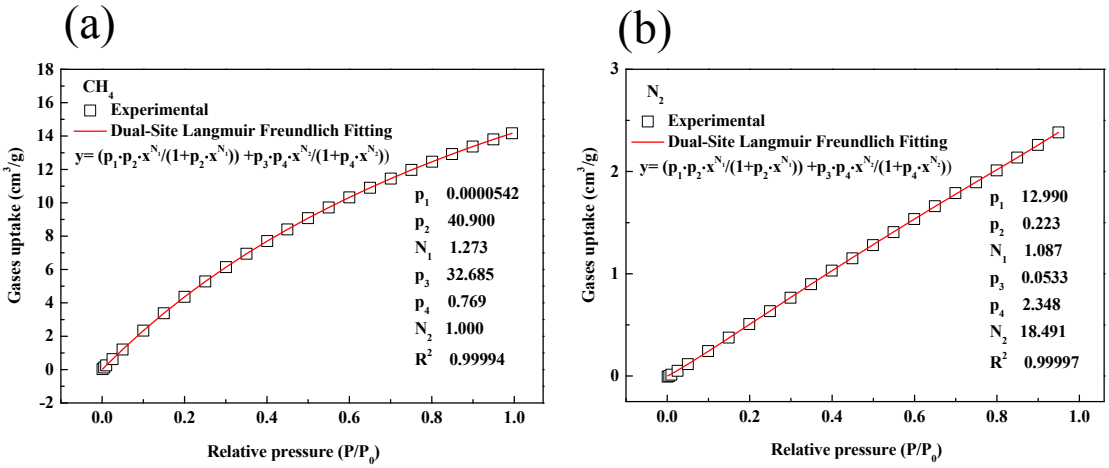

Figure S3. Fitting of the CH_4 (a) and N_2 (b) adsorption data of Cu-MOF at 298 K using dual-site Langmuir Freundlich model.

The pure single component isotherms of CH_4 and N_2 (CH_4 /N_2 (50/50, v/v)) at 298 K were fitted to the Toth equation：

$$y = N_{max} \times p_1 \times x/1 + \left((p_1 \times x^{p_2})^{1/P_2}\right)$$

$$K_H = N_{max} \times P_1$$

$$S_{i,j} = K_{H,i} / K_{H,j}$$

The ideal selectivity is about 10.94.

Table S4. The fitted parameters by using the Toth model based on the pure single-component isotherms data of CH_4 and N_2 in Cu-MOF at 298 K.

	298 K	
parameters	CH_4	N_2
N_{max}	1.46	0.263
P_1	0.769	0.391
P_2	1.000	2.707
R^2	0.99999	0.99994

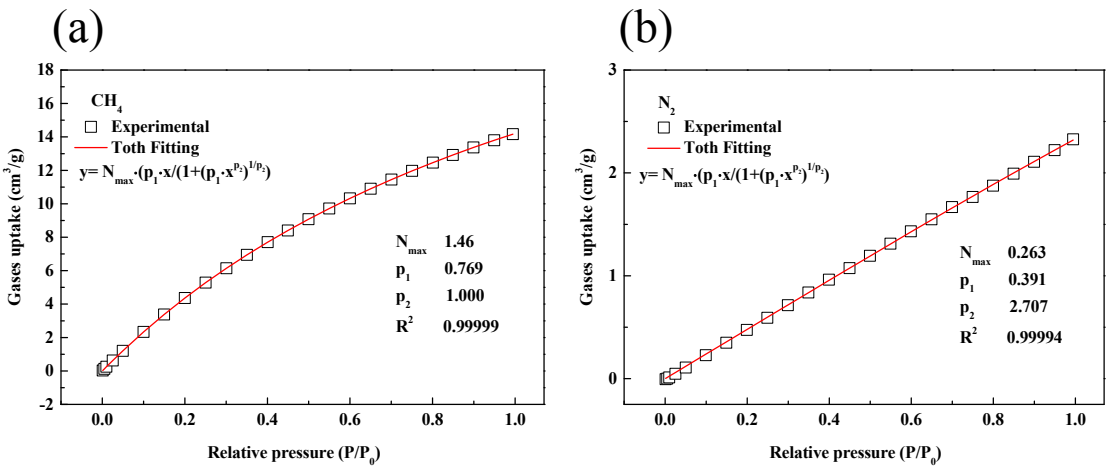

Figure S4. Fitting of the CH_4 (a) and N_2 (b) adsorption data of Cu-MOF at 298 K using Toth model.

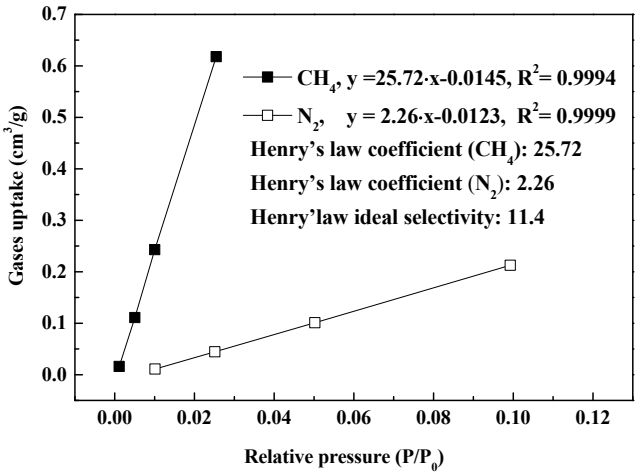

Figure S5. CH_4 and N_2 Henry's law coefficients and Henry's law ideal selectivity of Cu-MOF.

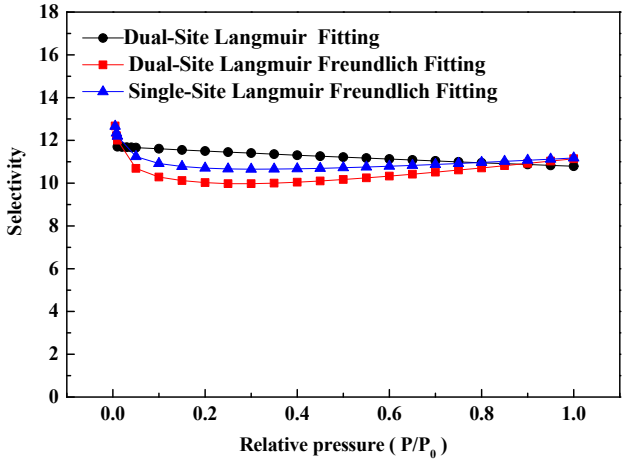

Figure S6. IAST-predicted selectivities using different fitting models.

S3. Characterization of MOFs

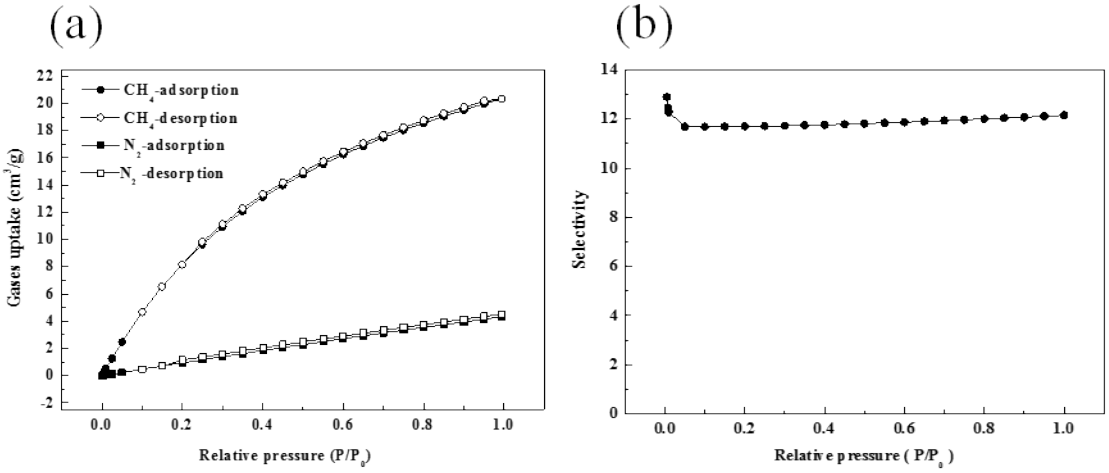

Figure S7. (a) Single component adsorption isotherms of CH_4 and N_2 in Cu-MOF at 273 K; (b) IAST selectivity of CH_4 and N_2 with equimolar mixture (CH_4 : N_2 = 0.5 : 0.5) at 273 K using dual-site Langmuir Freundlich model.

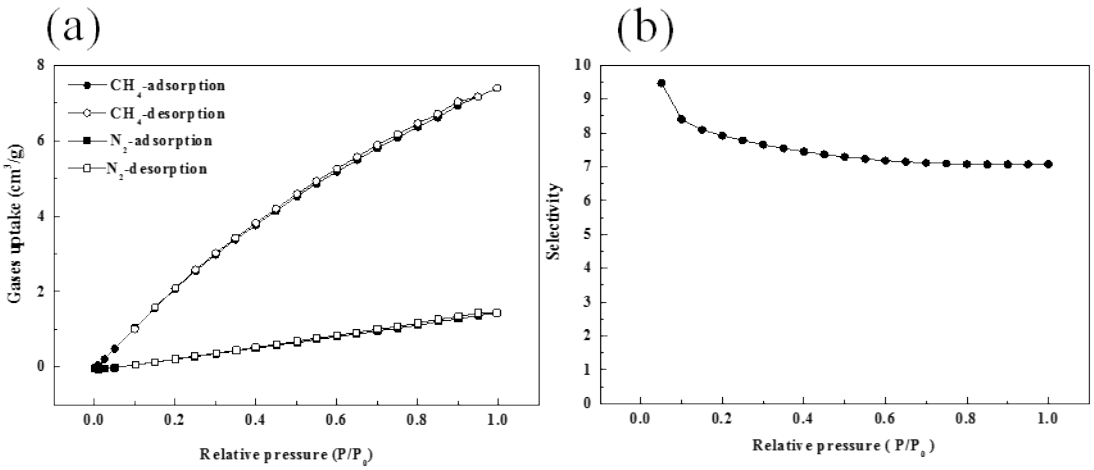

Figure S8. (a) Single component adsorption isotherms of CH_4 and N_2 in Cu-MOF at 323 K; (b) IAST predicted selectivity of equimolar CH_4/N_2 mixture at 323 K using dual-site Langmuir Freundlich model.

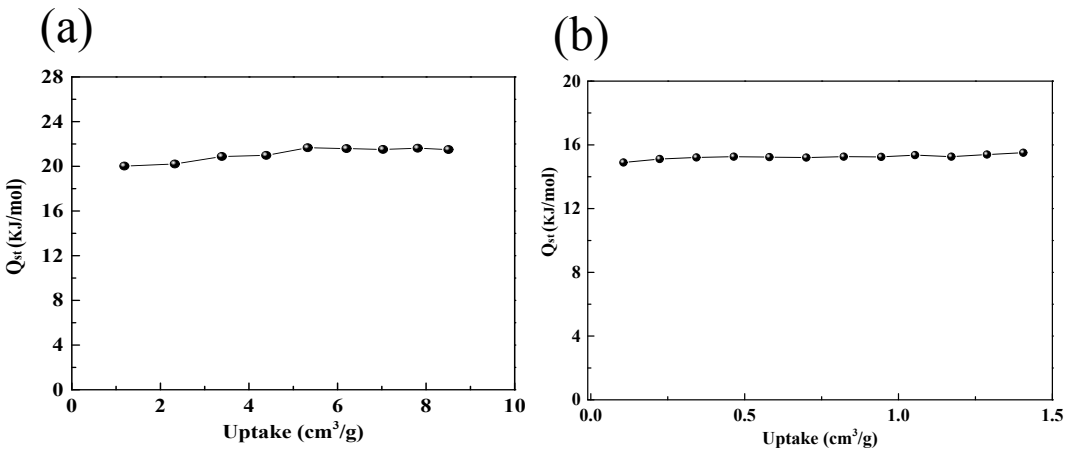

Figure S9. Adsorption heats of CH_4 (a) and N_2 (b) in Cu-MOF.

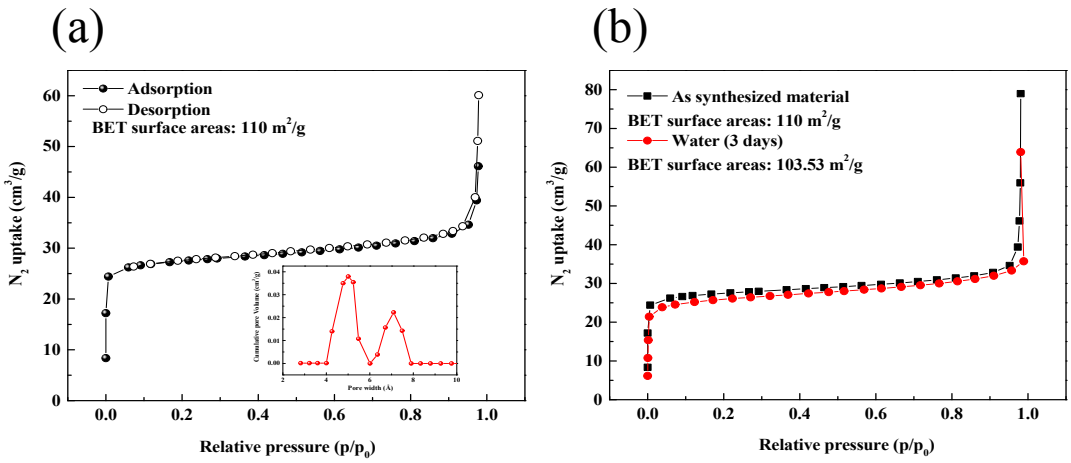

Figure S10. N_2 adsorption-desorption isotherm at 77 K (Inset: the pore size distribution) (a) and the BET surface areas after the treatment of the material using water (b) of Cu-MOF.

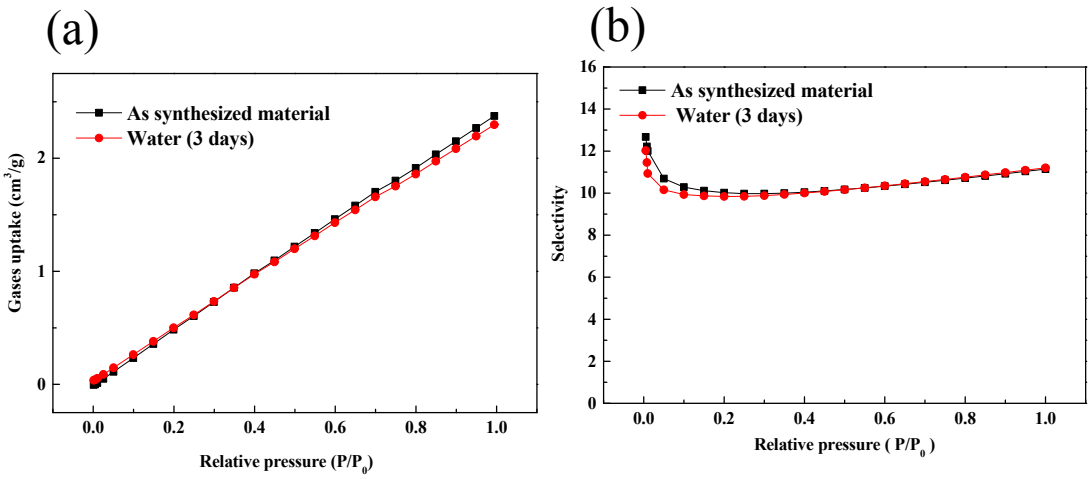

Figure S11. Adsorption capacity of N_2 after the treatment of the material using water (a) and the corresponding IAST selectivity of Cu-MOF using dual-site Langmuir Freundlich model (b).

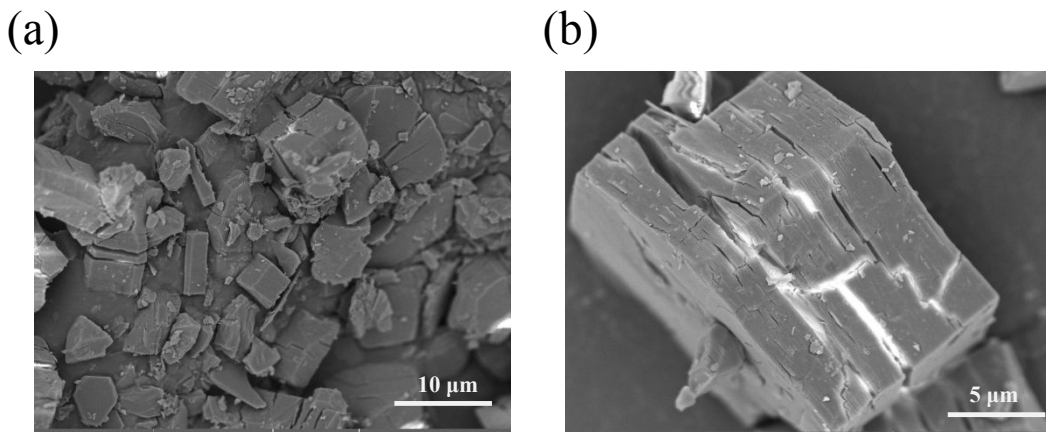

Figure S12. SEM pictures of Cu-MOF.

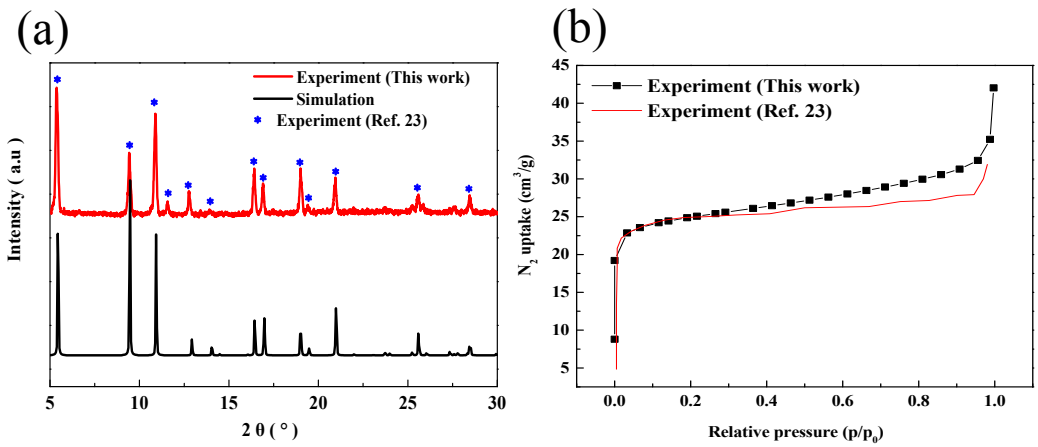

Figure S13. Power X-ray diffraction patterns (a) and N_2 adsorption-desorption isotherms at 77 K (b) of Cu-MOF.

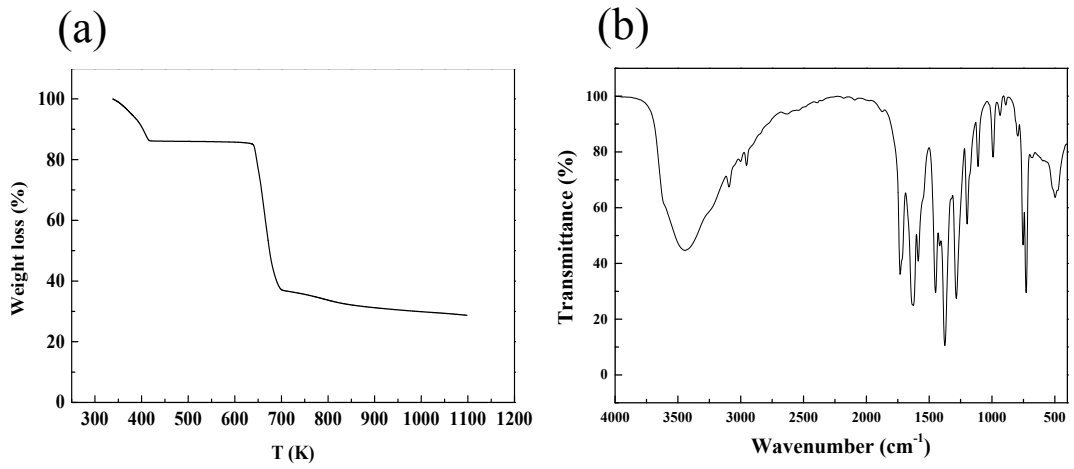

Figure S14. TGA curve (a) and FT-IR spectra (b) of Cu-MOF.

S4. Comparison with other porous materials

Table S5. Selectivity and adsorption heat of CH_4 and N_2 in different materials at 298 K and 1 bar.

Adsorbents	Selectivity for 50/50 CH_4/N_2 mixture	Q_{st} for CH_4 (kJ/mol)	Q_{st} for N_2 (kJ/mol)	Refs.
Co-MOF	12.5[a]	25.13	18.12	1
CTF-650	8.6[a]	27		2
Na-SAPO-34	2.6[b]	12.18	22.03	3
$[Ni_3(HCOO)_6]$	6.1[c]	24.82	19.33	4
$[Co_3(HCOO)_6]$	5.1[c]	23.03	19.7	4
Cu-BTC	3.69[c]	16.6	13.9	4
[Cu(Me-4py-trz-ia)]	4.2[a]	18	12	5
Basolite A100	3.7[a]	19	15.9	5
MOF-888	8.38[a]	26	22	6
MOF-889	6.41[a]	22	19	6
MOF-890	7[a]	23	19	6
MOF-891	7.78[a]	22	21	6
MOF-5	1.13[c]	12.2		7
MOF-177	4[c]	11.74		7
$Cu(OTf)_2$	4.8[a]	19.6	16	8
ZIF-68	3.5[a]	15.7[f]	11.9[f]	9
ZIF-69	3[a]	16.2[f]	12.8[f]	9
Ni-FA	6[a]	22.2	18	10
ZIF-8	2.8[d]	12.4[f]	9.8[f]	11
MIL-101-Cr	2.65[a] (293 K)	15 (293 K)	12 (293 K)	12
Cu(MOF)	6.9[a]	24	20	13
$[Cu(INA)_2]$	8.34[c]	17.52		14
Al-BDC	3.56[c]	18.74		14

Ni-HKUST-1	5.1[a]			15
Boron nitride	10[a]			16
$[Ni_3(HCOO)_6]$	6.18[c]			17
ATC-Cu	9.7[a]	26.8	16	18
ACF@$[Ni_3(HCOO)_6]$	6.22[c]			19
$[Cu(dhbc)_2(bpy)]$	2.2[e]			20
ZIF-68	3.89[c] (10 bar)	18.06 (10 bar)	14.58 (10 bar)	21
Cu-MOF	11.4[c]			This work
Cu-MOF	10.00-12.67[a]	20.02	15.04	This work

[a] Predicted by IAST.

[b] Mixture selectivity.

[c] Henry's law ideal selectivity.

[d] Calculated by theoretical calculations.

[e] the ratio of maximum uptake capacity.

[f] Obtained from calculations.

Co-MOF is $Co_3(C_4O_4)(OH)_2$.

Cu-BTC is $Cu_3(BTC)_2$, where BTC is 1,3,5-benzene tricarboxylate.

[Cu(Me-4py-trz-ia)], where Me-4py-trz-ia is 5-(3-methyl-5-(pyridin-4-yl)-4H-1,2,4-triazol-4-yl) isophthalate.

MOF-888, MOF-889, MOF-890 and MOF-891 are $[Ni_2(CPB)]$, $[Mg_2(CPB)(DEF)_{0.5}]$, $[Cu_3(CPB)(DMF)_{0.5}]$ and $[Cu_3(CPB)(DEF)_{0.4}]$, respectively, where CPB, DEF and DMF are 1′,2′,3′,4′,5′,6′-Hexakis(4-carboxyphenyl)benzene, N, N-Dimethylformamide and N, N-Diethylformamide, respectively.

MOF-5 is $[Zn_4O(BDC)]_n$, where BDC is 1,4-benzenedicarboxylate.

MOF-177 is $[Zn_4O(BTB)]_n$, where BTB is benzene tribenzoate.

$Cu(OTf)_2$, where OTf is trifluoromethanesulfonate.

ZIF-68 is $[Zn(bIM)_x(nIM)_y]_n$, where bIM and nIM are benzimidazole and 2-nitroimidazole, respectively.

ZIF-69 is $[Zn(cbIM)_x(nIM)_y]_n$, where cbIM and nIM are 5-chlorobenzimidazole and 2-nitroimidazole, respectively.

Ni-FA is $[Ni_3(HCOO)_6]$.

ZIF-8 is $[Zn(2\text{-}MI)]_n$, where 2-MI is 2-methylimidazole.

MIL-101-Cr is $[Cr_3F(H_2O)_2O[BDC]_3 \cdot nH_2O]_n$.

Cu(MOF) is $Cu(hfipbb)(H_2hfipbb)_{0.5}$, where $H_2hfipbb$ is 4, 4'-(hexafluoro isopropylidene)bis(benzoic acid).

$[Cu(INA)_2]_n$, where INA is isonicotinate.

Al-BDC is $[Al(BDC)(OH)]_n$.

Ni-HKUST-1 is $Ni_3(BTC)_2$.

ATC-Cu is $Cu_2(ATC)$, where ATC is 1, 3, 5, 7-adamantanetetracarboxylate.

$[Cu(dhbc)_2(bpy)]$, where dhbc and bpy are 2, 5-dihydroxybenzoic acid and 4, 4'-bipyridine, respectively.

Table S6. Uptake capacity, working capacity, ratio of working capacity and *SSP* values in different materials at 298 K and 1 bar.

Adsorbents	Uptake capacity of CH_4 (cm^3/g)	Working capacity of CH_4(cm^3/g)	Ratio of working capacity	*SSP* values	Refs
Co-MOF	9.03	1.51	0.506	6.32[a]	1
CTF-650	32.88	28.3	3.87	33[a]	2
Na-SAPO-34	13.44	11.2	1.95	5.08[b]	3
$[Ni_3(HCOO)_6]$	17.71	15.47	4.58	27.6[c]	4
$[Co_3(HCOO)_6]$	10.98	9.7	4.04	20.6[c]	4
Cu-BTC	20.41	17.38	2.48	9.16[a]	4
[Cu(Me-4py-trz-ia)]	25.09	21.05	3.57	15[a]	5
Basolite A100	16.58	13.21	3.84	14.21[a]	5
MOF-888	10.09	8.31	4.77	37.85[a]	6
MOF-889	25.98	22.30	4.85	31.15[a]	6
MOF-890	23.97	20.17	3.89	27.2[a]	6
MOF-891	29.99	24.72	4.42	32.41[a]	6
MOF-5	2.91	1.80	0.94	1.05[c]	7
MOF-177	12.61	8.81	3.78	15.12[c]	7
$[Cu(OTf)_2]$	5.69	5.10	2.01	9.6[a]	8
ZIF-68	8.96	8.02	2.91	10.2[a]	9
ZIF-69	11.2	10.10	3.36	10.08[a]	9
Ni-FA	17.92	18.9	4.42	26.56[a]	10
ZIF-8	4.48				11
MIL-101- Cr	14.56 (293 K)	10.6 (293K)	5.47(293K)	36.65[a] (293K)	12
Cu(MOF)	10.53	8.5	3.27	22.57[a]	13
$[Cu(INA)_2]$	17.90	15.80	5.5	40.16[c]	14
Al-BDC	16.31	14.50	3.34	11.9[c]	14
Ni-HKUST-1	37.49	31.49	4.03	20.56[a]	15
Boron nitride	14.78	13.90	3.2	32[a]	16
$[Ni_3(HCOO)_6]$	18.37	16.13	4.86	30.9[c]	17
ATC-Cu	64.96	47.28	3.04	40.9[a]	18
ACF@$[Ni_3(HCOO)_6]$	24.64	17.25	5.13	37[c]	19
$[Cu(dhbc)_2(bpy)]$	1.1				20
ZIF-68					21
Cu-MOF	14.17	11.4	5.90	65.73[a]	This work

[a] Calculated using IAST selectivity.

[b] Calculated using mixture selectivity.

[c] Calculated using Henry's law ideal selectivity.

References

(1) Li, L. Y.; Yang, L. F.; Wang, J. W.; Zhang, Z. G.; Yang, Q. W.; Yang, Y. W.; Ren, Q. L.; Bao, Z. B. Highly Efficient Separation of Methane from Nitrogen on a Squarate-Based Metal-Organic Framework. *AIChE J*. **2018**, *64*, 3681-3689.

(2) Yao, K. X.; Chen, Y. L.; Lu, Y.; Zhao, Y. F.; Ding, Y. Ultramicroporous carbon with extremely narrow pore distribution and very high nitrogen doping for efficient methane mixture gases upgrading. *Carbon*. **2017**, *122*, 258-265.

(3) Rivera-Ramos, M. E.; Hernández-Maldonado, A. J. Adsorption of N_2 and CH_4 by Ion-Exchanged Silicoaluminophosphate Nanoporous Sorbents: Interaction with Monovalent, Divalent, and Trivalent Cations. *Ind. Eng. Chem. Res*. **2007**, *46*, 4991-5002.

(4) Ren, X. Y.; Sun, T. J.; Hu, J. L.; Wang, S. D. Highly enhanced selectivity for the separation of CH_4 over N_2 on two ultra-microporous frameworks with multiple coordination modes. *Micropor. Mesopor. Mater*. **2014**, *186*, 137–145.

(5) Möllmer, J.; Lange, M.; Möller, A.; Patzschke, C.; Stein, K.; Läassig, D.; Lincke, J.; Gläser, R.; Krautscheid, H.; Staudt, R. Pure and mixed gas adsorption of CH_4 and N_2 on the metal–organic framework Basolite A100 and a novel copper-based 1,2,4-triazolyl isophthalate MOF. *J. Mater. Chem.* **2012**, *22*, 10274-10286.

(6) Nguyen, P. K.; Nguyen, H. D.; Pham, H. Q.; Kim, J.; Cordova, K. E.; Furukawa, H. Synthesis and Selective CO_2 Capture Properties of a Series of Hexatopic Linker-Based Metal−Organic Frameworks. *Inorg. Chem.* **2015**, *54*, 10065−10072.

(7) Saha, D.; Bao, Z. B.; Jia, F.; Deng, S. G. Adsorption of CO_2, CH_4, N_2O, and N_2 on MOF-5, MOF-177, and Zeolite 5A. *Environ. Sci. Technol.* **2010**, *44,* 1820-1826.

(8) Wang, X. Q.; Li, L. B.; Yang, J. F.; Li, J. P. CO_2/CH_4 and CH_4/N_2 separation on isomeric metal organic frameworks. *Chin. J. Chem. Eng*. **2016**, *24*, 1687–1694.

(9) Liu, B.; Smit, B. Molecular Simulation Studies of Separation of CO_2/N_2, CO_2/CH_4, and CH_4/N_2 by ZIFs. *J. Phys. Chem. C*. **2010**, *114*, 8515-8522.

(10) Liu, X. W.; Guo, Y.; Tao, A. D.; Fischer, M.; Sun, T. J.; Moghadam, P. Z.; Jimenez, D. F.; Wang, S. D. Explosive synthesis of metal-formate frameworks for methane capture: an experimental and computational study. *Chem. Commun*. **2017**, *53*, 11437-11440.

(11) Prez-Pellitero, J.; Amrouche, H.; Siperstein, F. R.; Pirngruber, G.; Nieto-Draghi, C.; Chaplais, G.; Simon-Masseron, A.; Bazer-Bachi, D.; Peralta, D.; Bats, N. Adsorption of CO_2, CH_4, and N_2 on Zeolitic Imidazolate Frameworks: Experiments and Simulations. *Chem. Eur. J.* **2010**, *16*, 1560-1571.

(12) Zhang, Y.; Su, W.; Sun, Y.; Liu, J.; Liu, X. W.; Wang, X. J. Adsorption Equilibrium of N_2, CH_4, and CO_2 on MIL-101. *J. Chem. Eng. Data.* **2015**, *60*, 2951-2957.

(13) Wu, X. F.; Yuan, B.; Bao, Z. B.; Deng, S. G. Adsorption of carbon dioxide, methane and nitrogen on an ultramicroporous copper metal–organic framework. *J. Colloid Interface Sci.* **2014**, *430*, 78-84.

(14) Hu, J. L.; Sun, T. J.; Liu, X. W.; Guo, Y.; Wang, S. D. Separation of CH_4/N_2 mixtures in metal–organic frameworks with 1D micro-channels. *RSC Adv*. **2016**, *6*, 64039–64046.

(15) Jia, X. X.; Yuan, N.; Wang, L.; Yang, J. F.; Li, J. P. $(CH_3)_2NH$-Assisted synthesis of high-purity Ni-HKUST-1 for the adsorption of CO_2, CH_4 and N_2. *Eur. J. Inorg. Chem*. **2018**, *2018*, 1047–1052.

(16) Saha, D.; Orkoulas, G.; Yohannan, S.; Ho, H. C.; Cakmak, E.; Chen, J. H.; Ozcan, S. Nanoporous boron nitride as exceptionally thermally stable adsorbent: role in efficient separation of light hydrocarbons. *ACS Appl. Mater. Interface*s. **2017**, *9*, 14506-14517.

(17) Guo, Y.; Hu, J. L.; Liu, X. W.; Sun, T. J.; Zhao, S. S.; Wang, S. D. Scalable solvent-free preparation of $[Ni_3(HCOO)_6]$ frameworks for highly efficient separation of CH_4 from N_2. *Chem. Eng. J*. **2017**, *327*, 564–572.

(18) Niu, Z.; Cui, X. L.; Pham, T.; Lan, P. C.; Xing, H. B.; Forrest, K. A.; Wojtas, L.; Space, B.; Ma, S. Q. A Metal–Organic Framework Based Methane Nano-trap for the Capture of Coal-Mine Methane. *Angew. Chem. Int. Ed.* **2019***,* DOI:10.1002/anie.201904507.

(19) Liu, X. W.; Hu, J. L.; Sun, T. J.; Guo, Y.; Bennett, T. D.; Ren, X. Y.; Wang, S. D. Template-based synthesis of a formate metal-organic framework/activated carbon fibre composite for high-performance methane adsorptive separation. *Chem-Asian J*. **2016**, *11*, 3014.

(20) Yang, J. F.; Yu, Q. H.; Zhao, Q.; Liang, J. M.; Dong, J. X.; Li, J. P. Adsorption CO_2, CH_4 and N_2 on two different spacing flexible layer MOFs. *Micropor. Mesopor. Mater.* **2012**, *161*, 154–159.

(21) Li, Q. Z.; Ruan, M. L.; Zheng, Y. N.; Mei, X. N.; Lin, B. Q. Investigation on the selective adsorption and separation properties of coal mine methane in ZIF-68 by molecular simulations. *Adsorption.* **2017**, *23*, 163–174.